

Article

Oil Quality Prediction in Olive Oil by Near-Infrared Spectroscopy: Applications in Olive Breeding

Hande Yılmaz-Düzyaman ^{1,*}, Raúl de la Rosa ^{2,*}, Leonardo Velasco ², Nieves Núñez-Sánchez ³
and Lorenzo León ¹

¹ IFAPA Centro Alameda del Obispo, Avda. Menéndez Pidal s/n, 14004 Córdoba, Spain; lorenzo.leon@juntadeandalucia.es

² Instituto de Agricultura Sostenible (CSIC), Avda. Menéndez Pidal s/n, 14004 Córdoba, Spain; lvelasco@ias.csic.es

³ Departamento de Producción Animal, Universidad de Córdoba, Campus de Rabanales, 14071 Córdoba, Spain; pa2nusan@uco.es

* Correspondence: hande.yilmaz@juntadeandalucia.es (H.Y.-D.); raul.rosa@ias.csic.es (R.d.l.R.)

Abstract: The oxidative stability index (OSI) and fatty acid (FA) composition of extra virgin olive oils (EVOOs) are key parameters in the characterization of new varieties in breeding programs. Their determination through traditional methods (Rancimat and gas chromatography, respectively) is expensive and time-consuming. Therefore, there is a need to develop rapid and cost-effective analytical procedures. This study aimed to evaluate the potential use of near-infrared spectroscopy (NIRS) for analyzing OSI and FA composition in EVOOs. A total of 318 samples sourced from different origins were evaluated using both FT-NIR MPA and MicroNIR instruments in transmittance mode, with wavelengths ranging from 1100 to 2500 nm and 908 to 1676 nm, respectively. Different accuracies were obtained in the models developed for the different evaluated traits, with simpler models (using a lower number of latent variables) for the MPA analyzer in all cases. Additionally, consistent results between instruments for the partitioning of the variance and heritability estimation, and the reliable ranking of genotypes were obtained from one of the sample sets tested. In summary, models derived from PLS regression using spectroscopic data of both instruments demonstrated promising results in determining these EVOO traits, facilitating their evaluation and selection of genotypes, particularly in breeding programs.

Keywords: olive breeding; EVOO; fatty acid composition; oxidative stability; comparative trials; near infrared; *Olea europaea*



Citation: Yılmaz-Düzyaman, H.; de la Rosa, R.; Velasco, L.; Núñez-Sánchez, N.; León, L. Oil Quality Prediction in Olive Oil by Near-Infrared Spectroscopy: Applications in Olive Breeding. *Agriculture* **2024**, *14*, 721. <https://doi.org/10.3390/agriculture14050721>

Academic Editor: Rodomiro Ortiz

Received: 4 April 2024

Revised: 29 April 2024

Accepted: 29 April 2024

Published: 2 May 2024



Copyright: © 2024 by the authors. Licensee MDPI, Basel, Switzerland. This article is an open access article distributed under the terms and conditions of the Creative Commons Attribution (CC BY) license (<https://creativecommons.org/licenses/by/4.0/>).

1. Introduction

Extra virgin olive oil (EVOO), a key component of the Mediterranean diet, is renowned for its various advantageous effects on human health, nutritional value, and remarkable sensory profile. These properties are attributed to its chemical composition, which presents distinctive characteristics compared with other vegetable oils. The saponifiable fraction, constituting a significant portion of the chemical composition of virgin olive oil (98%), is composed of triglycerides, glycerol esters, and fatty acids (FA), while the unsaponifiable fraction contains a small proportion of various essential compounds such as polyphenols, tocopherols (vitamin E), and chlorophyll [1,2]. The FA profile of EVOO is predominantly composed of monounsaturated fats, with oleic acid (C181) being the most common one, which are widely recognized as one of the healthiest dietary fat due to their capacity to improve cholesterol and promote cardiovascular health [2–4]. Furthermore, FA composition significantly influences the oxidative stability index (OSI) of olive oil, particularly the ratio of oleic to linoleic acid (C181/182), which is widely considered an EVOO quality indicator [5–7]. Therefore, OSI and FA composition are interrelated and are indirect indicators of the commercial, nutritional, and sensory properties of EVOO. Therefore, these quality

parameters are crucial in the characterization of new varieties in breeding programs. Their determination by traditional methods, Rancimat and gas chromatography, respectively, are time-consuming and produce waste. For instance, the Rancimat method allows only eight samples per day to be analyzed with a single instrument, and the cleaning of instrument accessories used in the analysis can be challenging. Therefore, with those traditional methods, it is not possible to analyze large numbers of genotypes in a breeding population and early-stage select for the OSI or FA content.

The use of near-infrared spectroscopy (NIRS) could represent an easier and faster non-destructive alternative for these analyses, enabling the rapid evaluation of numerous samples. NIRS is an analytical measurement technique that utilizes the near-infrared region of the electromagnetic spectrum with applications in many different products, including agri-food products [8].

From past to present, various spectroscopic techniques together with chemometric algorithms have been used for different purposes in analyzing olive samples such as leaves, fruits, and oils. Studies with visible and near-infrared reflectance spectroscopy have indicated that this method can be used to distinguish between young and adult olive leaves to facilitate breeding programs [9]. The FT-MIR technique was used with powders from leaves of five different Tunisian varieties and was reported to be 100% successful in differentiating cultivars [10]. In studies using the NIR method on intact olives, coefficients of determination higher than 80% were obtained for models regarding fruit moisture, oil content, C181, and C182 content [11,12]. In [13], the authors also concluded that FT-NIR methods are useful for estimating oil and moisture content in olive and olive pomace. NIRS, Vis/NIRS, and FT-NIR, in combination with an artificial neural network for the characterization of olives, estimating moisture content and controlling the oil elaboration process, gave promising results [14–17]. In [18], the authors highlighted the performance of the NIR method in detecting the quantification of adulteration of olive oil with almost 100% precision. Bellincontro et al. demonstrated that portable NIR-AOTF spectroscopy is an innovative, fast, and dependable approach for monitoring the oil accumulation [19] and prediction of phenolic compounds during the ripening process [20] in intact olive fruits in the field. Many studies with spectroscopic methods have been utilized to construct predictive models of various quality parameters of EVOO and other edible oils, such as OSI, FA compositions, peroxide index, squalene, conjugated dienes, alkyl and ethyl ester content, polyphenol content, color pigments, and chlorophyll [21–25]. However, NIRS has not been tested so far for its ability to accurately evaluate the quality parameters in a large number of oil samples needed in olive breeding programs.

For this reason, this study aims to evaluate the potential use of NIRS for the analysis of OSI and FA composition in EVOO and develop predictive models for estimating them with two cost-effective and rapid non-destructive NIR instruments. Full cross-validation models were analyzed to test whether the predicted results for those important quality components could be used as selection criteria in olive breeding programs, provided that the estimation of genetic parameters is consistent with reference methodologies.

2. Materials and Methods

2.1. Plant Materials

In this study, a total of 318 samples from different plant materials were used, including the core collection of the World Olive Germplasm Bank (WOGM) at IFAPA ‘Alameda del Obispo’ in Cordoba [26] and advanced selections from the IFAPA breeding program and cultivar comparative trials. Two kilograms of olive fruit samples were randomly handpicked from each elementary plot in different periods from mid-October to mid-November 2022. Following the harvest, the olive fruit samples were promptly transferred to the laboratory and refrigerated at 4 °C until olive oil extraction, which took place within 24 h.

2.2. Olive Oil Extraction

The extraction process was conducted with healthy and undamaged fruits. Olive oils were obtained using the Abencor system (Comercial Abengoa, S.A., Seville, Spain), a laboratory-scale version of an industrial olive oil mill consisting of a stainless hammer mill, thermo-mixer, and centrifuge. Initially, olive fruits were ground using a 5 mm sieve. Subsequently, 1.7 g of talc per 100 g of olive paste was added, followed by malaxation at 28 °C for 30 min. Finally, it was centrifuged at 3500 rpm for 2 min and left for approximately 2–3 h for decantation. The olive oils, filtered using qualitative filter paper, were stored in dark bottles at +4 °C until analysis.

2.3. Oxidative Stability Index

The OSI of the oils was evaluated using the Rancimat system (892 Professional Rancimat, Metrohm AG, Herisau, Switzerland). Each sample (2.5 g) was heated at 120 °C in the Rancimat apparatus with a continuous airflow of 20 L/h until a sudden increase in water conductivity occurred due to the adsorption of volatiles derived from oil oxidation. This period, known as induction time, was measured in hours.

2.4. Fatty Acid Composition

FA composition was analyzed by gas chromatography (GC) on a PerkinElmer Clarus 600 GC (PerkinElmer Inc., Waltham, MA, USA) equipped with a BPX70 30 m × 0.25 mm internal diameter × 0.25 µm film thickness capillary column (SGE Analytical Science Pty Ltd., Ringwood, Australia). Hydrogen was used as carrier gas at a constant flow of 0.8 mL/min. A split injector and flame ionization detector were maintained at 300 °C. The initial oven temperature was 140 °C, maintained for 2 min, followed by a rate increase of 20 °C/min up to 250 °C, maintained for 2 min. FA composition was calculated as % for each component. The main FAs, palmitic acid (C160), palmitoleic (C161), stearic acid (C180), oleic acid (C181), linoleic acid (C182), and linolenic acid (C183), and the ratio of oleic to linoleic acid (C181/182) were monitored in this work.

2.5. FT-NIR MPA and MicroNIR Measurements

FT-NIR MPA (Opus Bruker, Germany) and a portable MicroNIR™ Pro 1700 miniature spectrometer fitted with a liquid cell holder were used for this study. For FT-NIR MPA, spectral data were collected using Opus v. 7.5 software (Bruker Optik GmbH, Ettlingen, Germany). Olive oil spectra were collected in transmittance mode, and spectral data between 1100 and 2500 nm, every 2 nm, were used for chemometric analyses. For MicroNIR software, version 2.1 of Viavi Solutions Inc. (Santa Rosa, CA, USA) was used. Spectra were collected in the range of 908 to 1676 nm, with a resolution of 6.20 nm between points.

The acquisition of spectra was carried out by transmittance using disposable vial accessories for each instrument.

2.6. Data Analysis and Chemometrics

Unscrambler® X 10.4 software (CAMO A/S, Trondheim, Norway) was employed for the analysis of spectra from 318 olive oil samples. The baseline spectral correction of data was conducted initially and applied in all subsequent analyses. A wavelength range of 1100 to 2200 nm was utilized for FT-NIR MPA due to detector saturation beyond this range. For the MicroNIR, the wavelength range was 908 to 1676 nm. Various mathematical pretreatments, including multiplicative scatter correction and derivatives, were examined to enhance the predictive accuracy of the models.

Principal component analysis (PCA) was used to identify spectral outliers. Partial least squares (PLS) regression analysis was conducted using near-infrared spectral variables, with OSI and FA reference data as dependent variables, to develop predictive models.

The models' performance was assessed through full cross-validation, employing the leave-one-out method, and separate models were developed to estimate both OSI and FA for FT-NIR MPA and MicroNIR instruments. The correlations between actual and predicted

values, bias, and root mean square error of cross-validation were utilized to evaluate the performance of calibrations and cross-validation outcomes. The ratio of prediction to deviation (RPD), defined as the ratio of the standard deviation for any given constituent to the standard error of cross-validation or prediction for the same constituent, and the range error ratio (RER), defined as the ratio between the range of data for a specific constituent and the standard error of cross-validation or prediction for the same constituent, were also calculated to assess the relative effectiveness of each model [27].

Results from the core collection and comparative field trials were used to estimate genetic parameters and compare results of reference vs. NIR predicted from both instruments. In the core collection, 36 cultivars and 2–3 trees per cultivar were evaluated. The comparative field trials involved 4 cultivars ('Arbequina', 'Arbosana', 'Koroneiki', and 'Sikitita') in four environments in the provinces of Cordoba (with and without irrigation), Granada, and Jaen and three replicates of 30 plants per elementary plot. ANOVA of the reference and predicted data of OSI and FA was applied for variance component estimation from expected mean squares as similarly reported previously for fruit traits [28], according to the following statistical models:

For comparative field trials, $P_{ijk} = \mu + G_i + L_j + (G \times L)_{ij} + \varepsilon_{ijk}$, where P_{ijk} is the phenotypic value of k replication of the i genotype in the j location, μ is the overall mean, G_i is a random effect contributed by the i genotype, L_j is a random effect of the j location, $(G \times L)_{ij}$ is the interaction between the i genotype and the j location, and ε_{ijk} is the random residual error effect for the k measured replication. ANOVA provided the variance among genotypes (σ^2G) and among locations (σ^2L), associated with the genotype \times location interaction (σ^2GL), and the residual error effect for the measured samples ($\sigma^2\varepsilon$).

For the core collection, $P_{ij} = \mu + G_i + \varepsilon_{ij}$, where P_{ij} is the phenotypic value of j replication of the i genotype, μ is the overall mean, G_i is a random effect contributed by the i genotype, and ε_{ij} is the random residual error effect for the j measured replication. ANOVA provided the variance among genotypes (σ^2G) and the residual error effect for the measured samples ($\sigma^2\varepsilon$).

In both sets of data, the environmental variance for a genotype (σ^2E) was estimated, respectively, as $\sigma^2E = \sigma^2L/1 + \sigma^2GL/1 + \sigma^2\varepsilon/ls$, where l is the number of locations and s is the number of samples for comparative field trials, and $\sigma^2E = \sigma^2\varepsilon/s$, where s is the number of samples for the core collection. The broad-sense heritability of all studied traits was estimated as the ratio between the genotypic and the phenotypic variances: $H^2 = \sigma^2G/\sigma^2P = \sigma^2G/(\sigma^2G + \sigma^2E)$.

For genotypes of the core collection, Spearman correlation was also performed to compare the rankings of genotypes obtained from the reference and both MPA and MicroNIR instruments.

3. Results

3.1. Reference Data

Descriptive statistics and variability histograms were constructed for FA, including C181/182, C160, C161, C180, C181, C182, and C183, and for OSI (Table 1, Figure 1). The values of OSI and FA components exhibited distinct variability. The highest ranges of variations for the reference data were obtained from C181 and OSI values, with ranges of 41.04–84.57% and 0.40–38.73%, respectively. All reference data exhibited positive skewness, with the highest skewness observed in calculated C181/182 values, except for C181 (−1.31). Except for C181, C182, and the ratio of these two, the remaining reference values exhibited a normal distribution in terms of skewness. Likewise, positive kurtosis was observed for all reference data. Only OSI and C160 showed normal distribution in terms of kurtosis.

Table 1. Descriptive statistics for the oxidative stability index (OSI, h) and fatty acids (FA): ratio of oleic to linoleic acid (C181/182, %), palmitic acid (C160, %), palmitoleic (C161, %), stearic acid (C180, %), oleic acid (C181, %), linoleic acid (C182, %), and linolenic acid (C183, %).

	Mean	SD ¹	Minimum	Maximum	Skewness	Kurtosis
OSI	14.68	6.46	0.40	38.73	0.73	0.80
C160	15.46	2.82	8.73	23.65	0.16	0.08
C161	1.50	0.62	0.03	4.20	0.98	1.56
C180	2.54	0.56	0.00	4.70	0.35	1.27
C181	68.34	6.65	41.04	84.57	−1.31	2.62
C182	10.31	4.72	2.52	28.94	1.36	2.31
C183	0.81	0.23	0.00	1.86	0.31	2.21
C181/182	8.27	4.35	1.42	33.56	1.58	4.88

¹ SD: Standard deviation.

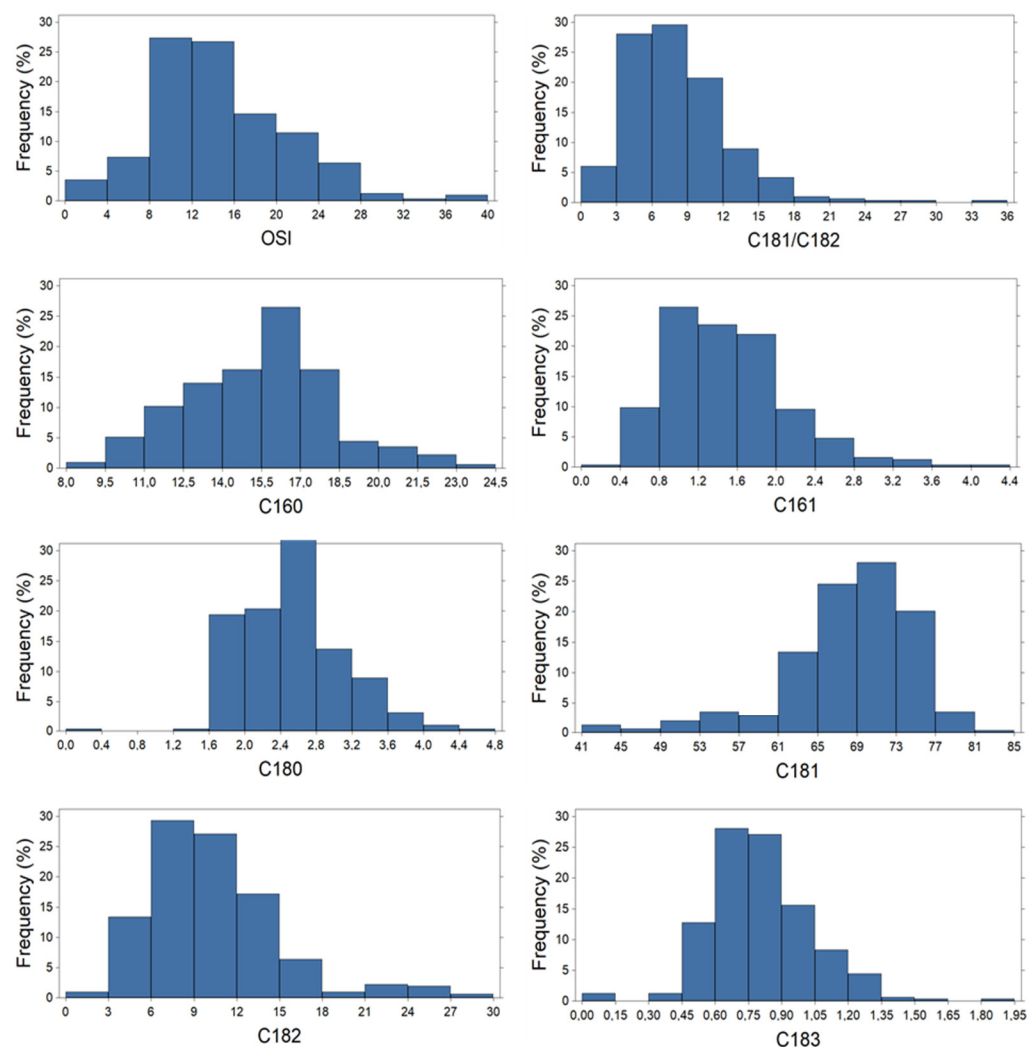


Figure 1. Histograms of variability for the oxidative stability index (OSI) and fatty acids (FA): ratio of oleic to linoleic acid (C181/182), palmitic acid (C160), palmitoleic (C161), stearic acid (C180), oleic acid (C181), linoleic acid (C182), and linolenic acid (C183).

3.2. Olive Oil Spectrum

The olive oil spectra obtained from the samples analyzed in this study are consistent with findings from prior studies [21,24,29–32]. The most prominent absorption peaks were detected at wavelengths of 1208 and 1390 nm for MicroNIR and, in addition to these, at wavelengths of 1726, 1762, and 2146 nm for the MPA instrument (Figure 2a,b). The spectral

region between 1090 and 1650 nm, where the spectra from the two instruments intersect, exhibits high similarity.

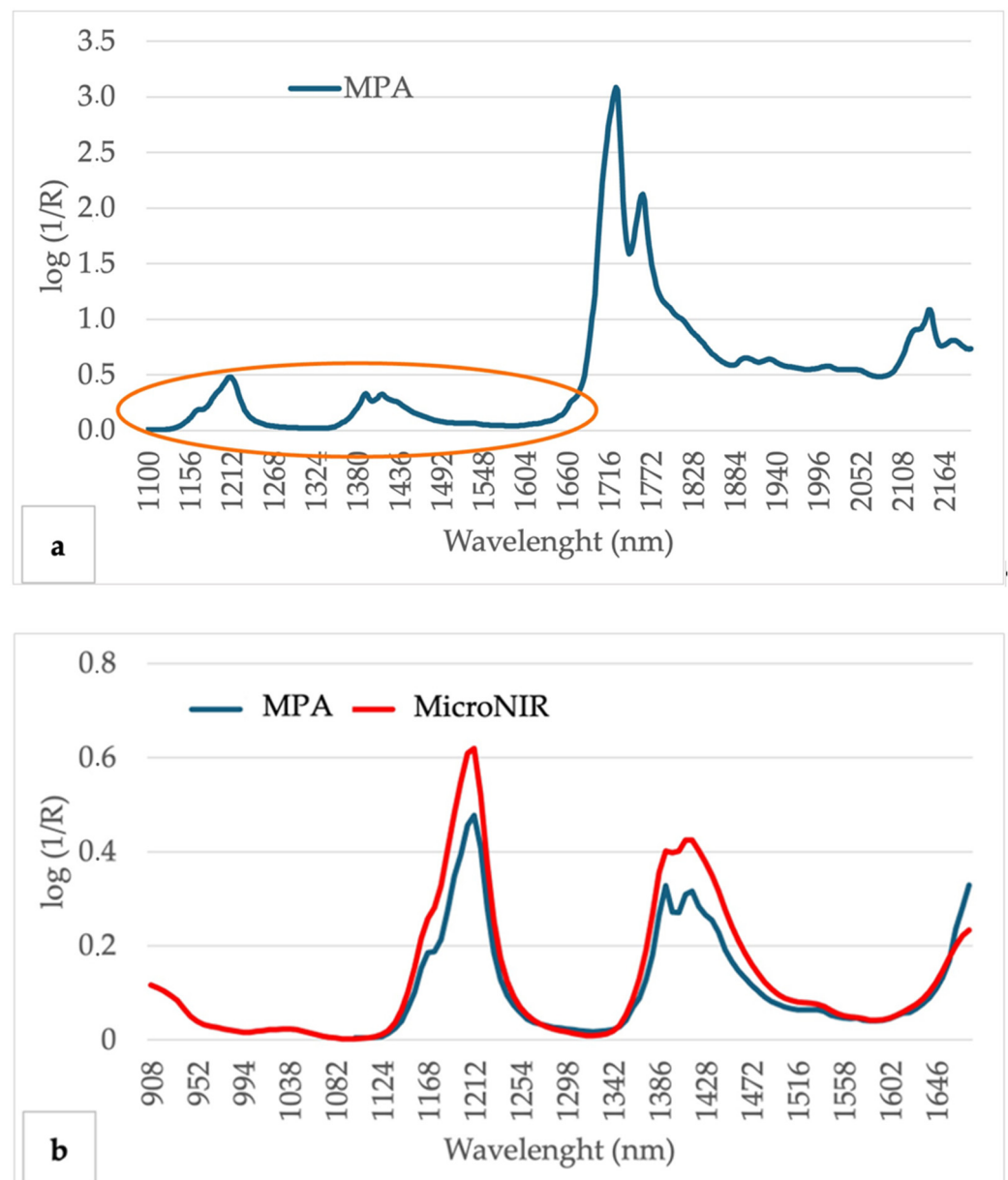


Figure 2. Average NIRS spectra of all olive oil samples: (a) with MPA detector and (b) with overlapped spectra fraction of MPA detector and MicroNIR.

3.3. Principal Component Analysis (PCA)

As an exploratory data analysis, PCA was performed on the full dataset for both instruments. The first two principal components of PCA explained 78% and 14%, and 65% and 30% of the total variance in MPA and MicroNIR, respectively. The score and influence plots from PCA allowed the identification of four samples with high leverage and a high residual in one or both instruments, and therefore, they were removed for further analysis as potential outliers' samples, i.e., samples poorly described and highly distant to model (Figures S1 and S2: Score and influence plot of the first two PCs obtained by PCA for 318 EVOO samples in MPA and MicroNIR). These four outlier samples showed distinctive higher absorbance across the entire wavelength region that could be attributed to differences in light scattering for these samples due to the decantation and filtration

processes. The rest of the analyses were conducted after removing these four outliers, resulting in a dataset comprising 314 samples.

3.4. Partial Least Squares (PLS) Regression Models

PLS regression models were constructed using absorbance data ranging from 1100 to 2192 nm for the MPA instrument and from 1100 to 1650 nm for MicroNIR, which were identified as the optimal ranges. The models were built using full cross-validation after excluding four outliers and realizing baseline correction. None of the other mathematical pretreatments tested significantly improved the prediction accuracy of the models.

The results are shown in Table 2 for both instruments. The best results in terms of R^2 , slope, RPD, and RER for both instruments were observed for C182, followed by C181. In addition, the number of PLS factors used in modeling these two components was considerably lower for MPA than for MicroNIR. In general, a lower number of factors were adequate for accurate modeling using the MPA instrument.

Table 2. Statistical parameters of cross-validation for the best models for predicting the oxidative stability index (OSI) and fatty acids (FA): ratio of oleic to linoleic acid (C181/182), palmitic acid (C160), palmitoleic (C161), stearic acid (C180), oleic acid (C181), linoleic acid (C182), and linolenic acid (C183).

	NPLS	RMSECV	R^2 CV	Slope	RPD	RER
MPA						
OSI	9	2.99	0.79	0.80	2.16	12.81
C160	9	1.25	0.80	0.81	2.26	11.92
C161	13	0.30	0.77	0.80	2.07	13.92
C180	14	0.33	0.67	0.69	1.70	14.41
C181	4	1.91	0.92	0.91	3.48	22.82
C182	3	0.83	0.97	0.97	5.69	31.91
C183	14	0.15	0.60	0.63	1.53	12.63
C181/182	3	2.43	0.69	0.70	1.79	13.23
MicroNIR						
OSI	14	3.14	0.76	0.79	2.06	12.20
C160	14	1.19	0.82	0.83	2.37	12.49
C161	20	0.35	0.69	0.74	1.77	12.02
C180	18	0.39	0.52	0.62	1.44	11.99
C181	10	1.60	0.94	0.94	4.16	27.28
C182	9	0.74	0.98	0.98	6.38	35.49
C183	16	0.18	0.39	0.50	1.28	10.24
C181/182	9	2.52	0.66	0.71	1.73	12.73

NPLS: number of factors used for PLS; RMSECV: root mean square error of cross-validation; R^2 CV: coefficient of determination of calibration and cross-validation, respectively; RPD: ratio of prediction to deviation; RER: range error ratio.

The regression coefficient plots provide an insight into the variables that contribute most to the model. Regression coefficients showed similar trends for all the components analyzed, with the main areas of influence corresponding to the main absorption peaks of EVOO. Thus, for instance, areas around 1750 and 2150 nm represent the highest values of regression coefficients for C181 and C182, in opposite directions due to the negative correlation between these components (Figure 3a). Regression coefficients of models for OSI also showed a similar pattern to C181, although other important spectral areas also contribute to this trait. Similar regression coefficients were also obtained for both instruments tested (Figure 3b), but regression coefficients were more clearly defined for MPA compared with MicroNIR.

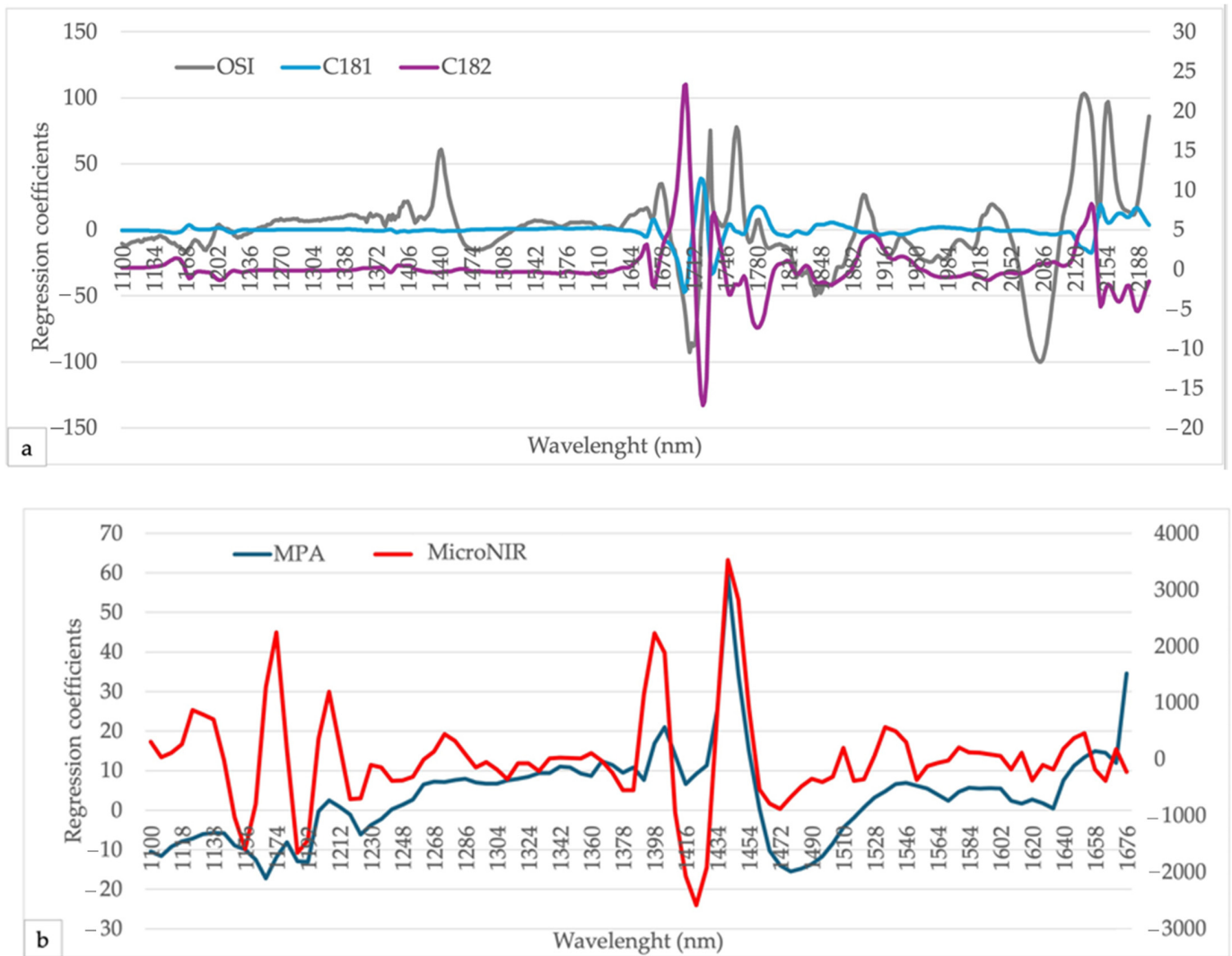


Figure 3. Regression coefficients of average NIRS spectra of all olive oil samples: (a) by OSI, C181, C182 with MPA detector and (b) by MPA detector and MicroNIR.

Predicted and reference scatter plots were generated for both instruments across all components. The plots reveal a consistent distribution of samples and a similar slope of regression lines for both MPA and MicroNIR instruments (Figure 4a–c).

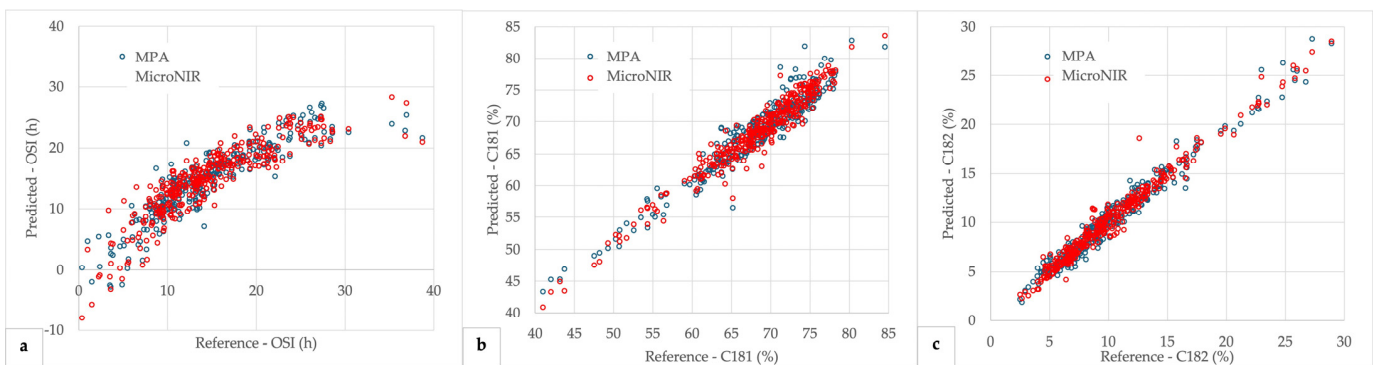


Figure 4. Predicted vs. reference plots from PLS models for both instruments MPA and MicroNIR: (a) for oxidative stability index (OSI, h), (b) for oleic acid (C181, %), and (c) for linoleic acid (C182, %).

However, models for the C181/C182 ratio showed less accurate models than expected according to individual models for its components. As can be inferred from scatter plots, linear regression does not seem to represent the best relationship between reference and predicted values for this character (Figure 5a). Indeed, a nonlinear asymptotic regression provided a much more accurate regression (Figure 5b). Thus, a high accuracy correlation for the C181/C182 ratio was also obtained when calculated from individual predicted values of its components (Figure 5c).

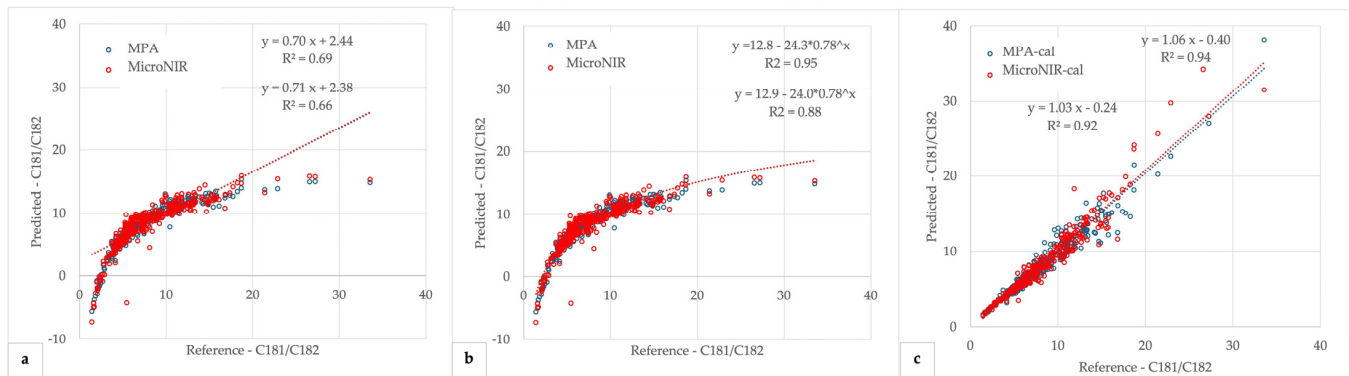


Figure 5. Predicted vs. reference plots from PLS models for both instruments MPA and MicroNIR for the C181/C182 ratio: (a) represented by linear regression, (b) represented by nonlinear asymptotic regression, and (c) represented by linear regression with data obtained from calculated individual predicted values.

ANOVA was conducted using reference values and predicted values of NIRS, followed by the calculation of variance components (genotype, environment, error) and H^2 for OSI and C181 for both instruments in the two sample sets evaluated (Tables 3 and 4). For comparative field trials, a more similar partitioning of the variance a H^2 estimation was found between reference and MPA predicted values, while different results were obtained for MicroNIR, which provided lower and higher estimates of H^2 for OSI and C181, respectively. For the core collection, the results for the partitioning of the variance a H^2 estimation were quite similar for all instruments and traits tested. Additionally, high and significant Spearman rank correlations were obtained in all cases.

Table 3. Variance components (%) and heritability (H^2) estimates from comparative field trials (Genotype x Environment, GxE) comparing reference vs. MPA and MicroNIR predicted values.

Trait	Instrument	Genotype	Environment	GxE	Error	H^2
OSI	Reference	61.00	26.19	2.66	10.14	0.78
	MPA	71.20	22.94	0.23	5.63	0.86
	MicroNIR	23.67	53.72	5.81	16.80	0.43
C181	Reference	54.90	38.31	1.83	4.96	0.79
	MPA	35.73	58.81	0.00	5.45	0.64
	MicroNIR	77.38	16.22	3.31	3.08	0.91

OSI: oxidative stability index; C181: oleic acid.

Table 4. Variance components (%) and heritability (H^2) estimates from core collection comparing reference vs. MPA and MicroNIR predicted values.

Trait	Instrument	Genotype	Error	H^2	r
OSI	Reference	90.39	9.61	0.90	
	MPA	87.67	12.33	0.88	0.87 ***
	MicroNIR	89.29	10.71	0.89	0.89 ***
C181	Reference	96.50	3.50	0.97	
	MPA	95.88	4.12	0.96	0.98 ***
	MicroNIR	94.37	5.63	0.94	0.98 ***

OSI: oxidative stability index; C181: oleic acid; r: Spearman rank correlation with reference data. *** significant at $p < 0.001$.

4. Discussion

In the present study, the potential use of NIRS to analyze OSI and FA composition in EVOO was tested by developing predictive models for estimating them with two cost-effective and rapid non-destructive NIR instruments. The comprehensive set of EVOO used in this study provided a wide variability for the traits of interest, wider than previously reported in other works. In [33], the author used a total of 172 reference data for modeling FA components, with C181 levels ranging from 56.54% to 79.50% (SD = 4.20) and C182 levels ranging from 3.86% to 21.92% (SD = 3.54). For OSI, a total of 192 reference data were used with a range of 1.33–18.55 h. In their study on FA conducted with 70 samples, the authors in [34] used a dataset of 70 olive oil values with a range of 58.90–77.90% (SD = 2.75) for C181 and 0–15.68% (SD = 2.95) for C182. In [21], the authors used a dataset of 147 samples for calibration with a range of 15.2–90.6 for OSI. In [35], the authors conducted a similar study on FA with 64 samples, obtaining reference values as follows: C181, 65.66–76.59%; C182, 4.90–15.12% (SD = 2.95); and OSI, 0.10–4.41 h. In [6], the authors obtained reference values from 82 samples for FA in their study as follows: C181, 56–80% (SD = 5); C182, 3–22% (SD = 4); and C181/C182, 3–25% (SD = 6). When comparing the reference data used in previous studies with that of this study, it is observed that the number of samples, the variations obtained, and the ranges of the reference values are lower. Although models have been developed to predict OSI and FA composition, comparing them is difficult due to differences in the reference methods and spectrometers used.

A prominent absorbance band centered at 1208 nm is indicative of the second overtone vibrations of C–H and CH = CH– bonds within the oil. Additionally, a significant shift in peak intensity at 1726 nm, associated with the stretching vibrations of the carbonyl C = O group found in the ester linkages between FA and the glycerol backbone present in oils and fats, aligns with findings from previous studies [25,31,32,36]. Spectral regions between 1300 and 1700 nm and 1800 and 2250 nm have been previously identified as most crucial for OSI models developed using NIRS [21]. In this study, the regression coefficients of the models for OSI also showed a similar pattern to C181. Still, other important spectral areas, such as 1300–1700 nm, also contribute to this feature, as noted in previous studies.

Several parameters were used to evaluate the performance of the calibrations developed. RMSECV aids in evaluating calibration model complexity by offering an average expected uncertainty for new samples and assisting in determining the optimal number of latent variables to minimize errors, while metrics such as correlation (R^2) and systematic deviation (bias) between predicted and actual values are also utilized to assess the quality of calibration models [31]. Previous research indicates that R^2 CV values ranging from 0.70 to 0.89 may be deemed indicative of good precision [24]. RPD values between 2 and 2.5 indicate that coarse quantitative predictions are possible, and values between 2.5 and 3 or above correspond to good and excellent prediction accuracy, respectively [37]. Finally, RER exceeding 4 is deemed acceptable for screening purposes in breeding programs, above 10 for quality control, and beyond 15 for quantification [27,38].

In the current study, excellent results were obtained for C181 and C182 with both MPA and MicroNIR instruments, and good results for all the other traits. In general, more simple

models were obtained for an MPA instrument compared with MicroNIR, with a lower number of PLS factors and more clearly defined regression coefficient plots. Mailer et al. [33] developed NIRS models for OSI with an R^2CV value of 0.83 and an SECV value of 0.973. Manley et al. [34] compared Büchi and PE spectra instruments and obtained R^2 values of 0.56 and 0.53; RPD values of 1.50 and 1.44, respectively, for C181; R^2 values of 0.88 and 0.90; and an RPD value of 2.81 for both instruments for C182. Cayuela-Sánchez et al. [21] reported an R^2CV value of 0.93 and an SEC value of 6.07 for OSI. Uncu et al. [35] obtained an R^2 value of 0.81 and an RMSECV value of 0.68 for OSI, an R^2 value of 0.81 and an RMSECV value of 0.97 for C181, and an R^2 value of 0.91 and an RMSECV value of 0.76 for C182. Milinovic et al. [6] reported R^2 values of 0.95, 0.99, and 0.86; RMSE values of 1.09, 0.43, and 2.09; and residual predictive deviations (RPD) of 4.5, 9.3, and 2.7 for C181, C182, and their ratio, respectively. As is well established, calibration studies benefit from a substantial sample size, yet merely increasing the sample count may not enhance calibration accuracy, particularly when values are closely clustered. Instead, the focus should be on ensuring a wide sample range and a uniform distribution [32,39]. While direct comparisons between studies are challenging due to methodological and equipment differences, it is noteworthy that our study incorporated the largest dataset of reference values. Additionally, it should be noted that none of the parameters used for testing the performance of the models and comparison with previous works should be considered as a universal, one-index-for-all-cases statistic allowing untroubled comparison across and between models [40].

In order to test a practical application of the model developed in olive breeding programs, an estimation of heritability was compared from the results obtained from each methodology. The ANOVA of the reference data for OSI and C181 indicates a predominant contribution of genotype, consistent with findings from prior research by using similar sample sets [41,42]. Different results were derived from NIRS-predicted values of both instruments according to the two sample sets tested. Thus, for comparative field trials, contrasting results were obtained for the partitioning of the variance a H^2 estimation for the evaluated traits. These results could be attributable to the limited number of genotypes and location tested compared with similar previous works for fruit traits [28]. Further analysis should be tested in future works in this direction with larger sample sets. However, for the core collection sample set, the results for the partitioning of the variance a H^2 estimation were highly consistent for all instruments and traits tested. Additionally, the high and significant Spearman rank correlations obtained in all cases indicates that a similar ranking of cultivars could be obtained from reference and the NIRS-predicted data from both instruments, and therefore, a confident selection of genotypes could be achieved from NIRS-predicted data. This is a crucial result for recommending the application of NIRS in olive breeding programs.

5. Conclusions

The objective of this study was to evaluate the potential use of near-infrared spectroscopy to analyze the OSI and FA composition in EVOO. In this study, high robustness was obtained in general for models developed with two instruments, with different accuracies for the different evaluated traits. These results allow the use of NIRS as an alternative to conventional reference methodologies, providing an easier and faster alternative for these analyses, in a non-destructive way and without using chemical reagents. A novel approach not previously explored in NIRS studies, to the best of the authors' knowledge, was tested from the comparison of heritability estimates from different instruments. Even though some contrasting results were obtained for the partitioning of the variance a H^2 estimation from one of the sample sets tested, the consistency of results and the reliable ranking of genotypes in the other sample set underscore the high usefulness of NIRS equipment for selection purposes, which could be particularly useful for the comparison of numerous genotypes in olive breeding programs.

Supplementary Materials: The following supporting information can be downloaded at <https://www.mdpi.com/article/10.3390/agriculture14050721/s1>, Figure S1: Score (a) and influence (b) plot of the first two PCs obtained by PCA for 318 EVOO samples in MPA, Figure S2: Score (a) and influence (b) plot of the first two PCs obtained by PCA for 318 EVOO samples in MicroNIR.

Author Contributions: Conceptualization, R.d.I.R., N.N.-S. and L.L.; data curation, H.Y.-D. and L.L.; funding acquisition, N.N.-S., L.V. and L.L.; methodology, H.Y.-D., L.V. and N.N.-S.; project administration, L.L.; writing—original draft, H.Y.-D.; writing—review and editing, H.Y.-D., R.d.I.R., L.V., N.N.-S. and L.L. All authors have read and agreed to the published version of the manuscript.

Funding: This research was partly funded through Grant PID2020-115853RR by MCIN/AEI/10.13039/501100011033. HYD is also grateful for the Predoctoral Contract Grant associated with the same project and ‘ESF investing in your future’.

Data Availability Statement: The data presented in this study are available on request from the corresponding author.

Acknowledgments: Special thanks to Angjelina Belaj, the curator of the World Olive Germplasm Bank of Córdoba (WOGBC).

Conflicts of Interest: The authors declare no conflicts of interest.

References

1. Servili, M.; Sordini, B.; Esposto, S.; Urbani, S.; Veneziani, G.; Di Maio, I.; Selvaggini, R.; Taticchi, A. Biological Activities of Phenolic Compounds of Extra Virgin Olive Oil. *Antioxidants* **2013**, *3*, 1–23. [[CrossRef](#)] [[PubMed](#)]
2. Gouvinhas, I.; Machado, N.; Sobreira, C.; Domínguez-Perles, R.; Gomes, S.; Rosa, E.; Barros, A. Critical Review on the Significance of Olive Phytochemicals in Plant Physiology and Human Health. *Molecules* **2017**, *22*, 1986. [[CrossRef](#)]
3. Kris-Etherton, P.M.; Pearson, T.A.; Wan, Y.; Hargrove, R.L.; Moriarty, K.; Fishell, V.; Etherton, T.D. High-Monounsaturated Fatty Acid Diets Lower Both Plasma Cholesterol and Triacylglycerol Concentrations. *Am. J. Clin. Nutr.* **1999**, *70*, 1009–1015. [[CrossRef](#)] [[PubMed](#)]
4. Visioli, F.; Galli, C. Olive Oil: More than Just Oleic Acid. *Am. J. Clin. Nutr.* **2000**, *72*, 853. [[CrossRef](#)] [[PubMed](#)]
5. Ceci, L.N.; Carelli, A.A. Relation Between Oxidative Stability and Composition in Argentinian Olive Oils. *J. Am. Oil Chem. Soc.* **2010**, *87*, 1189–1197. [[CrossRef](#)]
6. Milinovic, J.; Garcia, R.; Rato, A.E.; Cabrita, M.J. Rapid Assessment of Monovarietal Portuguese Extra Virgin Olive Oil's (EVOO's) Fatty Acids by Fourier-Transform Near-Infrared Spectroscopy (FT-NIRS). *Eur. J. Lipid Sci. Technol.* **2019**, *121*, 1800392. [[CrossRef](#)]
7. Emmanouilidou, M.G.; Koukourikou-Petridou, M.; Gerasopoulos, D.; Kyriacou, M.C. Oxidative Stability, Fatty-Acid and Phenolic Composition of Cypriot Monovarietal Virgin Olive Oils with Progressive Fruit Maturity. *J. Food Compos. Anal.* **2021**, *104*, 104191. [[CrossRef](#)]
8. Williams, P.; Norris, K. (Eds.) *Near-Infrared Technology in the Agricultural and Food Industries*; American Association of Cereal Chemists, Inc.: St. Paul, MN, USA, 1987; 330p.
9. León, L.; Downey, G. Preliminary studies by visible and near-infrared reflectance spectroscopy of juvenile and adult olive (*Olea europaea* L.) leaves. *J. Sci. Food Agric.* **2006**, *86*, 999–1004. [[CrossRef](#)]
10. Aouidi, F.; Dupuy, N.; Artaud, J.; Roussos, S.; Msallem, M.; Perraud-Gaime, I.; Hamdi, M. Discrimination of Five Tunisian Cultivars by Mid InfraRed Spectroscopy Combined with Chemometric Analyses of Olive *Olea Europaea* Leaves. *Food Chemistry* **2012**, *131*, 360–366. [[CrossRef](#)]
11. León, L.; Garrido-Varo, A.; Downey, G. Parent and Harvest Year Effects on Near-Infrared Reflectance Spectroscopic Analysis of Olive (*Olea Europaea* L.) Fruit Traits. *J. Agric. Food Chem.* **2004**, *52*, 4957–4962. [[CrossRef](#)]
12. León, L.; Rallo, L. Análisis de aceituna intacta mediante espectroscopía en el infrarrojo cercano (NIRS): Una herramienta de utilidad en programas de mejora de olivo. *Grasas y Aceites* **2003**, *54*, 41–47. [[CrossRef](#)]
13. Barros, A.S.; Nunes, A.; Martins, J.; Delgado, I. Determination of Oil and Water in Olive and Olive Pomace by NIR and Multivariate Analysis. *Sens. Instrum. Food Qual.* **2009**, *3*, 180–186. [[CrossRef](#)]
14. Bendini, A.; Cerretani, L.; Carrasco-Pancorbo, A.; Gómez-Caravaca, A.M.; Segura-Carretero, A.; Fernández-Gutiérrez, A.; Lercker, G. Phenolic Molecules in Virgin Olive Oils: A Survey of Their Sensory Properties, Health Effects, Antioxidant Activity and Analytical Methods. An Overview of the Last Decade Alessandra. *Molecules* **2007**, *12*, 1679–1719. [[CrossRef](#)] [[PubMed](#)]
15. Cayuela, J.A.; García, J.M.; García, J.M.; Caliani, N.; Caliani, N. NIR Prediction of Fruit Moisture, Free Acidity and Oil Content in Intact Olives. *Grasas y Aceites* **2009**, *60*, 194–202. [[CrossRef](#)]
16. Cayuela, J.A.; Camino, M.D.C.P. Prediction of Quality of Intact Olives by near Infrared Spectroscopy. *Eur. J. Lipid Sci. Technol.* **2010**, *112*, 1209–1217. [[CrossRef](#)]
17. Allouche, Y.; López, E.F.; Maza, G.B.; Márquez, A.J. Near Infrared Spectroscopy and Artificial Neural Network to Characterise Olive Fruit and Oil Online for Process Optimisation. *J. Near Infrared Spectrosc.* **2015**, *23*, 111–121. [[CrossRef](#)]

18. Christy, A.A.; Kasemsumran, S.; Du, Y.; Ozaki, Y. The Detection and Quantification of Adulteration in Olive Oil by Near-Infrared Spectroscopy and Chemometrics. *Anal. Sci.* **2004**, *20*, 935–940. [[CrossRef](#)]
19. Bellincontro, A.; Caruso, G.; Mencarelli, F.; Gucci, R. Oil Accumulation in Intact Olive Fruits Measured by near Infrared Spectroscopy–Acousto-optically Tunable Filter. *J. Sci. Food Agric.* **2013**, *93*, 1259–1265. [[CrossRef](#)]
20. Bellincontro, A.; Taticchi, A.; Servili, M.; Esposto, S.; Farinelli, D.; Mencarelli, F. Feasible Application of a Portable NIR-AOTF Tool for On-Field Prediction of Phenolic Compounds during the Ripening of Olives for Oil Production. *J. Agric. Food Chem.* **2012**, *60*, 2665–2673. [[CrossRef](#)]
21. Cayuela Sánchez, J.A.; Moreda, W.; García, J.M. Rapid Determination of Olive Oil Oxidative Stability and Its Major Quality Parameters Using Vis/NIR Transmittance Spectroscopy. *J. Agric. Food Chem.* **2013**, *61*, 8056–8062. [[CrossRef](#)]
22. Cayuela, J.A.; Yousfi, K.; Carmen Martínez, M.; García, J.M. Rapid Determination of Olive Oil Chlorophylls and Carotenoids by Using Visible Spectroscopy. *J. Am. Oil Chem. Soc.* **2014**, *91*, 1677–1684. [[CrossRef](#)]
23. Cayuela, J.A. Rapid NIR Determination of Alkyl Esters in Virgin Olive Oil. *Grasas y Aceites* **2017**, *68*, 195. [[CrossRef](#)]
24. Garrido-Varo, A.; Sánchez, M.-T.; De La Haba, M.-J.; Torres, I.; Pérez-Marín, D. Fast, Low-Cost and Non-Destructive Physico-Chemical Analysis of Virgin Olive Oils Using Near-Infrared Reflectance Spectroscopy. *Sensors* **2017**, *17*, 2642. [[CrossRef](#)] [[PubMed](#)]
25. Cayuela, J.A.; García, J.F. Sorting Olive Oil Based on Alpha-Tocopherol and Total Tocopherol Content Using near-Infra-Red Spectroscopy (NIRS) Analysis. *J. Food Eng.* **2017**, *202*, 79–88. [[CrossRef](#)]
26. Belaj, A.; Dominguez-García, M.D.C.; Atienza, S.G.; Martín Urdíroz, N.; De la Rosa, R.; Satovic, Z.; Martín, A.; Kilian, A.; Trujillo, I.; Valpuesta, V.; et al. Developing a Core Collection of Olive (*Olea Europaea* L.) Based on Molecular Markers (DARs, SSRs, SNPs) and Agronomic Traits. *Tree Genet. Genomes* **2012**, *8*, 365–378. [[CrossRef](#)]
27. Williams, P.C.; Sobering, D.C. Comparison of Commercial near Infrared Transmittance and Reflectance Instruments for Analysis of Whole Grains and Seeds. *J. Near Infrared Spectrosc.* **1993**, *1*, 25–32. [[CrossRef](#)]
28. León, L.; Velasco, L.; de la Rosa, R. Initial Selection Steps in Olive Breeding Programs. *Euphytica* **2015**, *201*, 453–462. [[CrossRef](#)]
29. Armenta, S.; Garrigues, S.; De La Guardia, M. Determination of Edible Oil Parameters by near Infrared Spectrometry. *Anal. Chim. Acta* **2007**, *596*, 330–337. [[CrossRef](#)] [[PubMed](#)]
30. Nenadis, N.; Tsikouras, I.; Xenikakis, P.; Tsimidou, M.Z. Fourier Transform Mid-infrared Spectroscopy Evaluation of Early Stages of Virgin Olive Oil Autoxidation. *Eur. J. Lipid Sci. Technol.* **2013**, *115*, 526–534. [[CrossRef](#)]
31. Sikorska, E.; Khmelinskii, I.; Sikorski, M. Vibrational and Electronic Spectroscopy and Chemometrics in Analysis of Edible Oils. In *Methods in Food Analysis*; Cruz, R.M.S., Khmelinskii, I., Vieira, M., Eds.; CRC Press: Boca Raton, FL, USA, 2016; pp. 211–244. ISBN 978-0-429-06983-3.
32. García Martín, J.F. Potential of Near-Infrared Spectroscopy for the Determination of Olive Oil Quality. *Sensors* **2022**, *22*, 2831. [[CrossRef](#)]
33. Mailer, R.J. Rapid Evaluation of Olive Oil Quality by NIR Reflectance Spectroscopy. *J. Am. Oil Chem. Soc.* **2004**, *81*, 823–827. [[CrossRef](#)]
34. Manley, M.; Eberle, K. Comparison of Fourier Transform near Infrared Spectroscopy Partial Least Square Regression Models for South African Extra Virgin Olive Oil Using Spectra Collected on Two Spectrophotometers at Different Resolutions and Path Lengths. *J. Near Infrared Spectrosc.* **2006**, *14*, 111–126. [[CrossRef](#)]
35. Uncu, O.; Ozen, B. Prediction of Various Chemical Parameters of Olive Oils with Fourier Transform Infrared Spectroscopy. *LWT–Food Sci. Technol.* **2015**, *63*, 978–984. [[CrossRef](#)]
36. Eldin, A.B. Near Infra Red Spectroscopy. In *Wide Spectra of Quality Control*; IntechOpen: London, UK, 2011. [[CrossRef](#)]
37. Nicolai, B.M.; Beullens, K.; Bobelyn, E.; Peirs, A.; Saeys, W.; Theron, K.I.; Lammertyn, J. Nondestructive Measurement of Fruit and Vegetable Quality by Means of NIR Spectroscopy: A Review. *Postharvest Biol. Technol.* **2007**, *46*, 99–118. [[CrossRef](#)]
38. Sim, J.; McGoverin, C.; Oey, I.; Frew, R.; Kebede, B. Near-Infrared Reflectance Spectroscopy Accurately Predicted Isotope and Elemental Compositions for Origin Traceability of Coffee. *Food Chem.* **2023**, *427*, 136695. [[CrossRef](#)] [[PubMed](#)]
39. Fearn, T. Flat or natural? A note on the choice of calibration samples. In *Near Infra-Red Spectroscopy: Bridging the Gap between Data Analysis and NIR Applications*; Hildrum, K.I., Isaksson, T., Naes, T., Tandberg, A., Eds.; Ellis Horwood Ltd.: Chichester, UK, 1992; pp. 61–66.
40. Esbensen, K.H.; Geladi, P.; Larsen, A. Mythbusters in Chemometrics. *NIR News* **2012**, *23*, 19–21. [[CrossRef](#)]
41. Serrano, A.; De La Rosa, R.; Sánchez-Ortiz, A.; Cano, J.; Pérez, A.G.; Sanz, C.; Arias-Calderón, R.; Velasco, L.; León, L. Chemical Components Influencing Oxidative Stability and Sensorial Properties of Extra Virgin Olive Oil and Effect of Genotype and Location on Their Expression. *LWT* **2021**, *136*, 110257. [[CrossRef](#)]
42. Navas-López, J.F.; Cano, J.; de la Rosa, R.; Velasco, L.; León, L. Genotype by Environment Interaction for Oil Quality Components in Olive Tree. *Eur. J. Agron.* **2020**, *119*, 126115. [[CrossRef](#)]

Disclaimer/Publisher’s Note: The statements, opinions and data contained in all publications are solely those of the individual author(s) and contributor(s) and not of MDPI and/or the editor(s). MDPI and/or the editor(s) disclaim responsibility for any injury to people or property resulting from any ideas, methods, instructions or products referred to in the content.